Electronic Supplementary Material (ESI)

The Mechanisms of HSA@PDA/Fe Nanocomposites Enhanced Nanozyme Activity and Their Application for the Intracellular H_2O_2 Detection

Xiaofeng Liu, Jinan Qin, Xiaoyu Zhang, Liyuan Zou, Xiaohai Yang, Qing Wang, Yan Zheng, Wenjing Mei and Kemin Wang**

State Key Laboratory of Chemo/Biosensing and Chemometrics, College of Chemistry and Chemical Engineering, Key Laboratory for Bio-Nanotechnology and Molecular Engineering of Hunan Province, Hunan University, Changsha 410082, China.

* E-mail address: wwqq99@hnu.edu.cn, kmwang@hnu.edu.cn; Tel/Fax: +86-731-88821566.

Table of Contents

Section A. Materials and characterizations

Materials and Reagents. Human serum albumin (HSA), bovine serum albumin (BSA), lysozyme (LSZ), glucose oxidase (GOx), peroxidase from horseradish (HRP), 3,3',5,5'-tetramethylbenzidine (TMB), luminol, 2,2'-azinobis-(3-ethylbenzthiazoline-6-sulphonate) (ABTS) and 3-(4,5-dimethylthiazol-2-yl)-2-diphenyltetrazolium bromide (MTT) were obtained from Sigma-Aldrich (St. Louis, MO). $FeCl_3 \cdot 6H_2O$ was purchased from Sinopharm Chemical Reagent Co., Ltd. (Shanghai, China). Dopamine hydrochloride and phorbol-12-myristate-13-acetate (PMA) were purchased from J&K Scientific Ltd. (Beijing, China). The copper sulfate pentahydrate ($CuSO_4 \cdot 5H_2O$), and other salt reagents were commercially obtained from Dingguo Biotechnology Co., Ltd. (Beijing, China). Polyetherimide (PEI) was purchased from Sangon Biotech. Co., Ltd. (Shanghai, China). All the chemical reagents were of analytical grade and used without further purification. Ultrapure water (18.2 MΩ·cm) was used to prepare all reagents in the experiments.

Characterizations. To evaluate the morphology of the samples, the samples for transmission electron microscope (TEM) analysis were prepared by drying a drop of aqueous solution of HSA@PDA/Fe nanocomposites. on a copper grid and observed by Tecnai G2 F20 S-TWIN (FEI, Holland). Dynamic light scattering (DLS) and Zeta potential of HSA@PDA/Fe nanocomposites were also per-formed using a Zeta-sizer Nano ZS90 (Malvern Instruments, UK). In addition, X-ray Photoelectron Spectroscopy (XPS) was used for the characterization of chemical composition and state of elements present in the HSA@PDA/Fe nanocomposites. The materials (HSA@PDA, PDA/Fe nanocomposites and HSA@PDA/Fe nanocomposites) were dried and analyzed by XPS ESCALAB 250Xi (Thermo Fisher Scientific, USA). The ultraviolet-visible (UV-vis)

absorption spectra were recorded on spectrophotometer UV-2600 (Shimadzu, Japan). Electron paramagnetic resonance measurement was carried out using a JES-FA200 EPR spectrometer (JEOL, Japan) at ambient temperature. Fourier transform infrared (FTIR) spectra were performed using TENSOR27 Spectrometer (Bruker, Germany).

Section B. Experimental section

Synthesis of Materials: HSA@PDA/Fe nanocomposites were synthesized using a simple method. In brief, dopamine (10 mg) and HSA (10 mg) was dissolved in 9 mL ultrapure water under magnetic stirring which eventually formed a homogenous solution for 30 min and adjusted pH values (5 to 10). Then, 1 mL $FeCl_3 \cdot 6H_2O$ (4.9 mg/mL) solution was added and the magnetic stirring was continued for 6 h. HSA@PDA nanocomposites were synthesized under the same conditions without the addition of $FeCl_3 \cdot 6H_2O$. Similarly, PDA/Fe nanocomposites were synthesized under the same conditions without the addition of HSA. The product was washed with ultrapure water for three times and lyophilized for further use. In addition, BSA@PDA/Fe and LSZ@PDA/Fe nanocomposites were synthesized using the same method with HSA@PDA/Fe nanocomposites, only changing HSA into BSA and LSZ, respectively.

Kinetic Analysis: The mixture of the substrates with specific concentrations and H_2O_2 in buffer solution was catalyzed by fixed concentration of Fe^{3+}, HSA@PDA/Fe Nanocomposites, BSA@PDA/Fe and LSZ@PDA/Fe nanocomposites. The reaction solution include H_2O_2 (1 mM) and TMB with variable concentration of 1 μM, 2.5 μM, 5 μM, 10 μM, 25 μM and 50 μM. The total volume of the reaction mixture was 400 μL. All of the experiments were conducted in 10 mM HAc-NaAc buffer, pH = 4.5, the absorbance at 652 nm. The products were confirmed using UV-vis spectrophotometer and the concentrations of products were calculated by their molar extinction coefficients ε at respective wavelengths. All the experiments were done for three times. The reaction rates were fitted to Michaelis Menten equation:

$v=V_{max} \times ([S])/([S]+K_M)$

The K_M value was a constant, which reflected the binding affinity between enzymes and substrates. The V_{max} value revealed the turnover number of enzymes and reflected their biocatalytic activity.

Analysis of Peroxidase-Like Activity: Typically, 10 μL HSA@PDA/Fe nanocomposites (400 μg/mL) was introduced into 280 μL HAc-NaAc buffer (10 mM, pH 4.5), followed by the addition of 100 μL TMB solution (4 mM) and 10 μL H_2O_2 (40 mM). The catalytic oxidation of TMB was followed spectroscopically by measuring the absorbance at 652 nm.

Stability measurements: Stabilities of HSA@PDA/Fe nanocomposites and HRP enzyme were determined in HAc-NaAc buffer at different conditions. The assay consisted of the following steps:, 10 μL HSA@PDA/Fe nanocomposites (400 μg/mL) was introduced into 280 μL HAc-NaAc buffer (10 mM), followed by the addition of 100 μL TMB solution (4 mM) and 10 μL H_2O_2 (40 mM). The catalytic oxidation of TMB was followed spectroscopically by measuring the absorbance at 652 nm. Relative activities were calculated from the ratio of residual activity to the original activity before incubation. The effect of pH or temperature on the peroxidase-like activity of HSA@PDA/Fe nanocomposites was also investigated by the above assay. In addition, to further demonstrate the stability of HSA@PDA/Fe nanocomposites, the freeze-thawing (-20 ℃) and thermal (80 ℃) cycle assay for HSA@PDA/Fe nanocomposites and HRP enzyme were testified. The HSA@PDA/Fe nanocomposites after freeze-thawing and thermal cycle assay were introduced the reaction solution including 280 μL HAc-NaAc buffer (10 mM, pH 4.5), followed by the addition of 100 μL TMB

solution (4 mM) and 10 μL H_2O_2 (40 mM). Relative activities were calculated by referring to the above steps.

Detection of hydroxyl radical (•OH): The determination of •OH was characterized by electron paramagnetic resonance (EPR) device. The steps were as follows: the HAc-NaAc buffer (pH 4.5, 10 mM) contained 25 mM 2,2,6,6-Tetramethyl-1-piperidinyloxy (TEMPO), 20 μg/ mL^{-1} HSA@PDA/Fe nanocomposites and 100 μM H_2O_2, was prepared. After incubation of 5 min, EPR spectra were recorded.

ABTS Oxidation by HSA@PDA/Fe Nanocomposites: A typical ABTS oxidation reaction mixture included 10 μL (400 μg/mL), 70 μL HAc-NaAc buffer (10 mM, pH 4.5), 10 μL of variable concentrations of ABTS. Subsequently, 10 μL of H_2O_2 (10 mM) were added to the different reaction mixtures. The catalytic oxidation of ABTS was followed spectroscopically by measuring the absorbance at 418 nm.

HSA@PDA/Fe Nanocomposites Catalyzed Generation of Chemiluminescence: In a typical experiment, 10 μL HSA@PDA/Fe nanocomposites (200 μg/mL), 70 μL Tris-HCl buffer (10 mM, pH = 8.0), 10 μL containing variable concentrations of luminol and 10 μL H_2O_2 (10 mM) were mixed. The catalytic oxidation of luminol was followed spectroscopically by measuring the generated chemiluminescence using Fluorescence Spectrophotometer.

Detection of the Yield of Fe(II) by Reduction of Fe(III) by HSA@PDA/Fe Nanocomposites: To evaluate the conversion efficiency of Fe^{3+} into Fe^{2+} ions, 1.10-phenanthroline monohydrate (1 mg/mL) was used as the color-developing agent (ortho-

phenanthroline photometry). HSA@PDA/Fe nanocomposites and H_2O_2 (1 mM) were added into the solution. Then 50 μL of solution was taken out and mixed with 1,10-phenanthroline monohydrate every 5 min. The absorbance intensity was characterized by UV-vis spectroscopy for analysis of the corresponding amount of Fe^{2+} ions.

Determination of H_2O_2: 10 μL HSA@PDA/Fe nanocomposites (400 μg/mL) was introduced into 280 μL HAc-NaAc buffer (10 mM, pH 4.5), followed by the addition of 100 μL TMB solution (4 mM) and 10 μL H_2O_2 with varying concentration (0-2.5 mM). The mixture was incubated at 37 °C for 10 min with continuous oscillation. The final reaction solution was used to perform the absorption spectroscopy measurement.

Cell Viability Assay: MTT assays were carried out to evaluate the potential cytotoxicity of the proposed probes and lipofectamine to the cells. MCF-7 cells were seeded in a 96-well plate at a density of 1×10^5 cells per well in a total volume of 200 μL. The plates were maintained in a humidified atmosphere with 5% CO_2 at 37 °C. After overnight incubation, the original incubating medium was discarded. Fresh media containing HSA@PDA/Fe nanocomposites (0, 0.5, 1, 2, 5, 10 and 50 μg/mL) or TMB (0, 0.05, 0.1, 0.2, 0.5, 1 and 2 mM) were added to the MCF-7 cells and incubated for 24 h, 10 μL of MTT solution (5 mg/mL) was added to each well with incubation at 37 °C for 4h. Finally, 150 μL of DMSO was added to dissolve the precipitated formazan violet crystals. The cell viability was determined by measuring the absorbance at 490 nm by a multidetection microplate reader.

In Situ Detection of H_2O_2 Released from ~~MCF-7~~ Cells: To evaluated the H_2O_2 released from MCF-7 and SMCC-7721 cells, the cells were dropped into the 96-

microwell plates for 24 h. After that, the plates were washed three times using PBS solution. Then, the PMA solutions (20 μL, 0, 0.5, 1, 1.5, 2 and 3 μM) and 50 μL of PBS were added successively and incubated 30 min. Finally, HSA@PDA/Fe nanocomposites (200 μg/mL, 10 μL), TMB (50 μL, 4 mM), and 70 μL HAc-NaAc buffer (10 mM, pH 4.5) were added subsequently for incubation 10 min. Finally, the absorbances at 652 nm were recorded by a multidetection microplate reader.

Section C. Results and discussion

Table S1. Comparison of the kinetic parameters of HSA@PDA/Fe nanocomposites, Fe^{3+}-MCNs, Fe_3O_4 NPs, Fe^{3+}, GO-COOH, CQDs, Carbon nanohorn, $C_{60}[C(COOH)_2]_2$ and HRP with H_2O_2 as the substrate. K_M is the Michaelis constant and V_{max} is the maximal reaction rate.

Catalyst	Substrate	K_m (mM)	V_{max} ($M\ s^{-1}$)	Reference
HSA@PDA/Fe nanocomposites	H_2O_2	0.129	3.72×10^{-7}	This work
Fe^{3+}-MCNs	H_2O_2	161	6.76×10^{-9}	1
Fe_3O_4 NPs	H_2O_2	154	9.78×10^{-8}	2
Fe^{3+}	H_2O_2	247	9.26×10^{-10}	This work
GO-COOH	H_2O_2	3.99	3.85×10^{-8}	3
CQDs	H_2O_2	26.77	3.06×10^{-7}	4
Carbon nanohorn	H_2O_2	49.80	2.07×10^{-8}	5
$C_{60}[C(COOH)_2]_2$	H_2O_2	24.58	4.01×10^{-8}	6
HRP	H_2O_2	3.7	8.71×10^{-8}	2
Pt nanoparticles	H_2O_2	0.12	1.30×10^{-6}	7
B-rGO nonosheets	H_2O_2	11	2.63×10^{-6}	8
Co_3O_4 cubes	H_2O_2	140	1.20×10^{-7}	9
PMCS	H_2O_2	40.16	1.22×10^{-7}	10
FeN_5 SA/CNF	H_2O_2	0.148	7.58×10^{-6}	11

Table S2. Comparison of the kinetic parameters of HSA@PDA/FeNCs, BSA-PDA-FeNCs, Lysozyme-PDA-FeNCs, Fe_3O_4 NPs, and HRP with TMB as the substrate. K_M is the Michaelis constant and Vmax is the maximal reaction rate.

Catalyst	Substrate	K_m (mM)	V_{max} ($M\ s^{-1}$)	Reference
HSA@PDA/FeNCs	TMB	1.201	5.18×10^{-8}	This work
BSA-PDA-FeNCs	TMB	0.585	8.73×10^{-8}	This work
Lysozyme-PDA-FeNCs	TMB	0.030	3.50×10^{-8}	This work
Fe_3O_4 NPs	TMB	0.098	3.44×10^{-8}	2
HRP	TMB	0.434	1.00×10^{-7}	7

Table S3. Comparison with other nanozymes for H_2O_2 detection by colorimetric method.

Method	Liner range (μM)	Detection limit (μM)	Reference
MoS_2 nanosheets	5-100	1.5	12
3D graphene/Fe_3O_4-Au NPs	20-190	12	13
Cu(HBTC)-1/Fe_3O_4-Au NPs	2.86-71.43	1.10	14
$CeVO_4$-2 NR	1-250	70	15
FeHPO	57.4-525.8	1.0	16
GO-Fe_3O_4	1-50	0.3	17
HPPtCuDs	0.3-325	0.1	18
$Ce(OH)CO_3$	0-80	0.3	19
CA-BiPt NC/GO	0.01-1500	0.01	20
HSA@PDA/Fe nanocomposites	0.5-100	0.06	This work

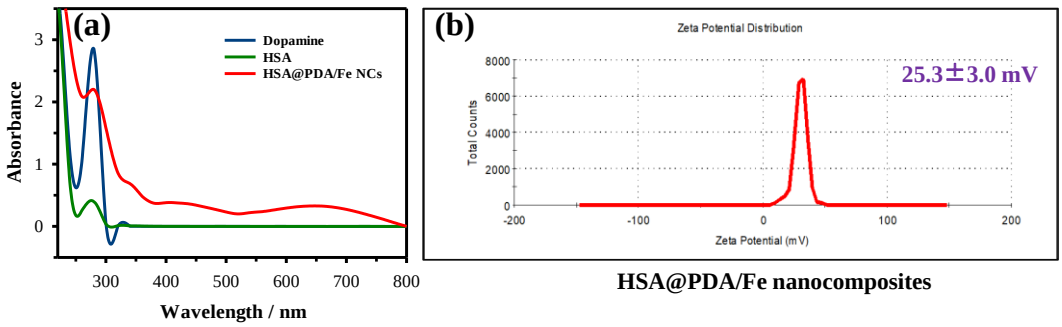

Fig. S1 Formation of HSA@PDA/Fe nanocomposites. A) The absorbance spectra of DA, HSA and HSA@PDA/Fe nanocomposites, B) The Zeta potential measurements of HSA@PDA/Fe nanocomposites.

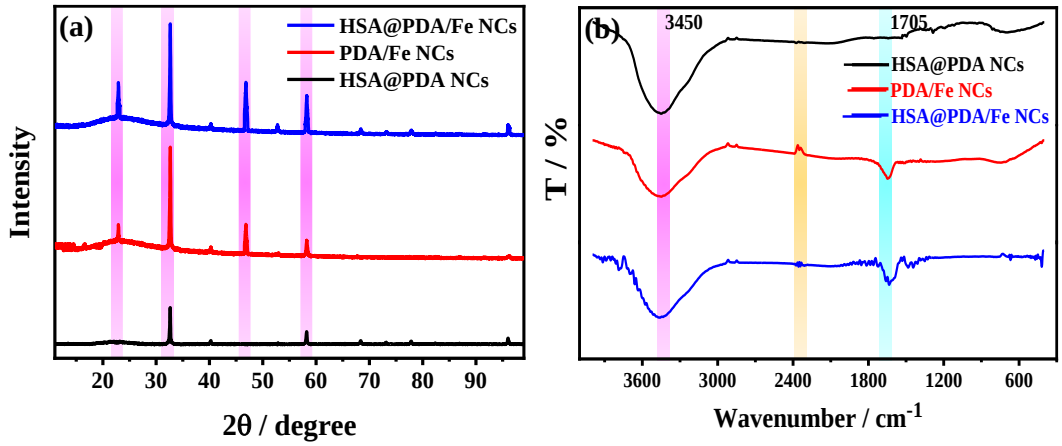

Fig. S2 XRD patterns (a) and FTIR spectra (b) of HSA@PDA, PDA/Fe nanocomposites and HSA@PDA/Fe nanocomposites.

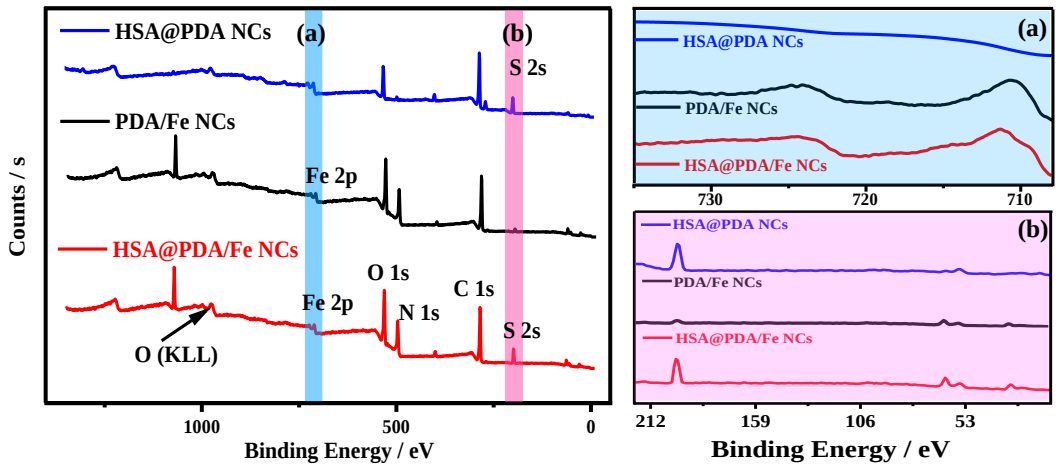

Fig. S3 XPS spectra of HSA@PDA, PDA/Fe nanocomposites and HSA@PDA/Fe nanocomposites.

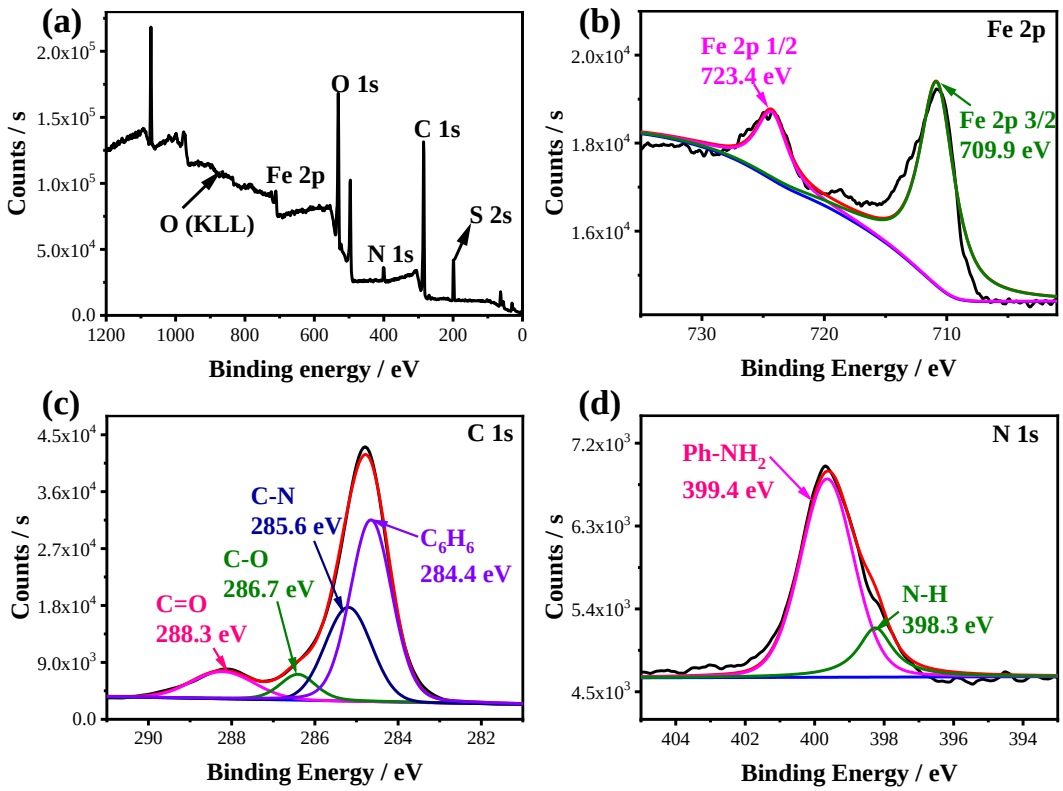

Fig. S4 (a) The XPS pattern of HSA@PDA/Fe NCs. (b) The high-resolution XPS pattern of Fe 2p. (c) The high-resolution XPS pattern of C 1s. (d) The high-resolution XPS pattern of N 1s.

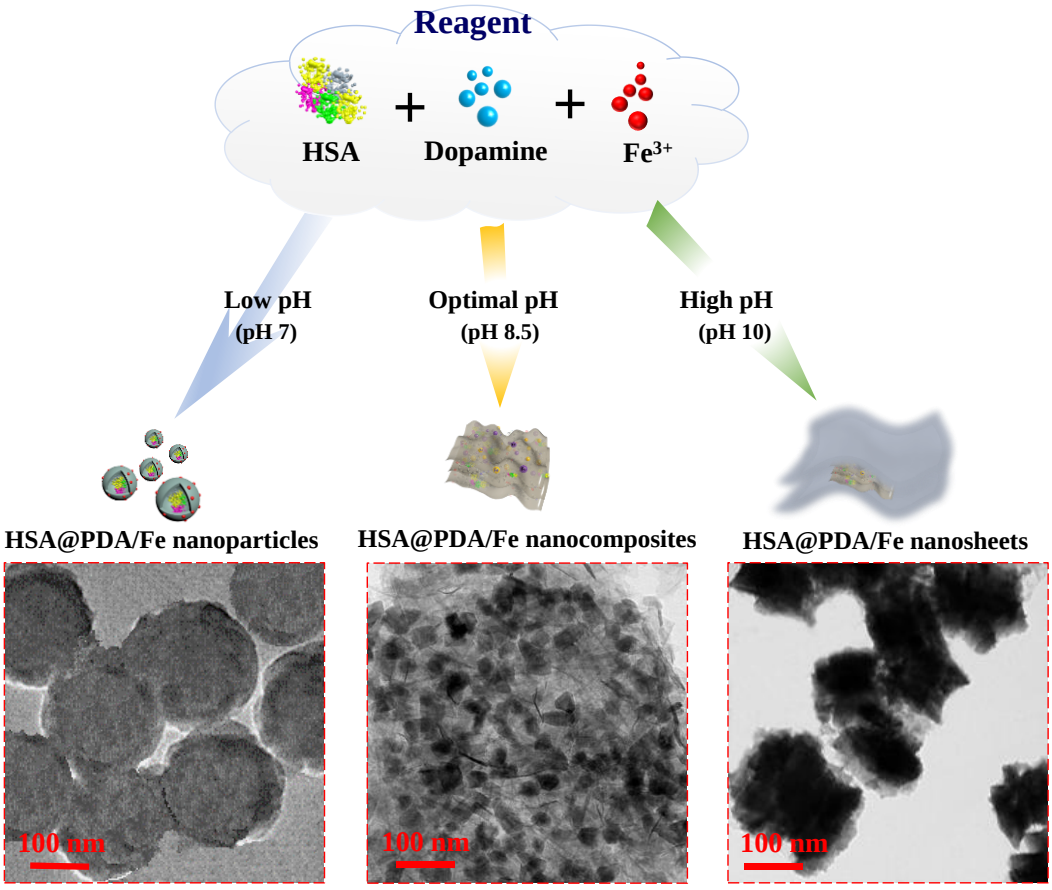

Fig. S5 The influence of pH on the morphology ~~and catalytic performance~~ of HSA@PDA/Fe nanocomposites was directly suggested by TEM images. Scale bars were 100 nm.

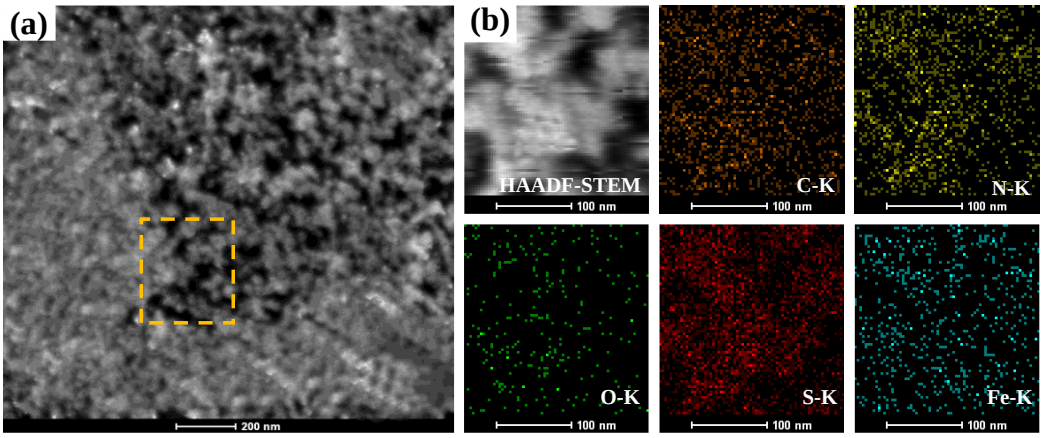

Fig. S6 The high-angle annular dark-field (HAADF)-STEM image of HSA@PDA/Fe nanocomposites in low pH values (pH 7), and corresponding TEM element mappings of the C, N, O, S and Fe-K edge signals. Scale bars are 100 nm.

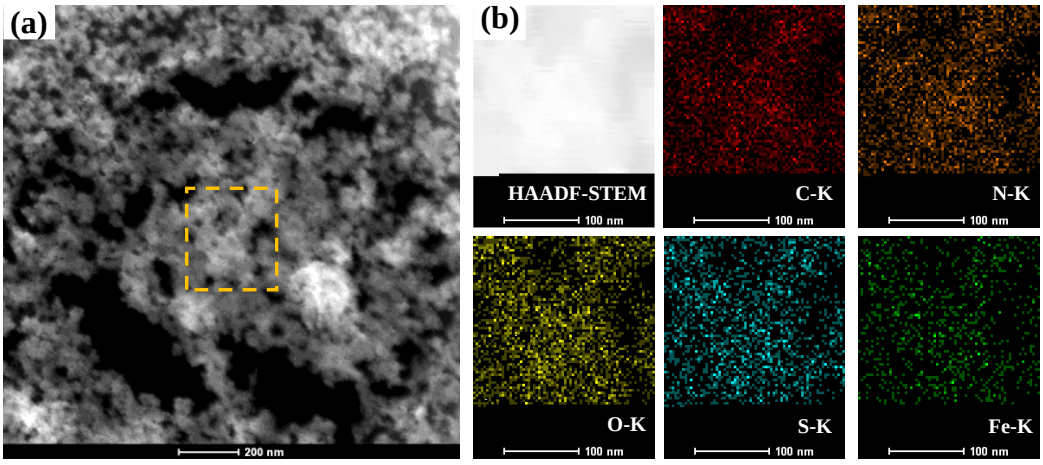

Fig. S7 The HAADF-STEM image of HSA@PDA/Fe nanocomposites in high pH values (pH 10), and corresponding TEM element mappings of the C, N, O, S and Fe-K edge signals. Scale bars are 100 nm.

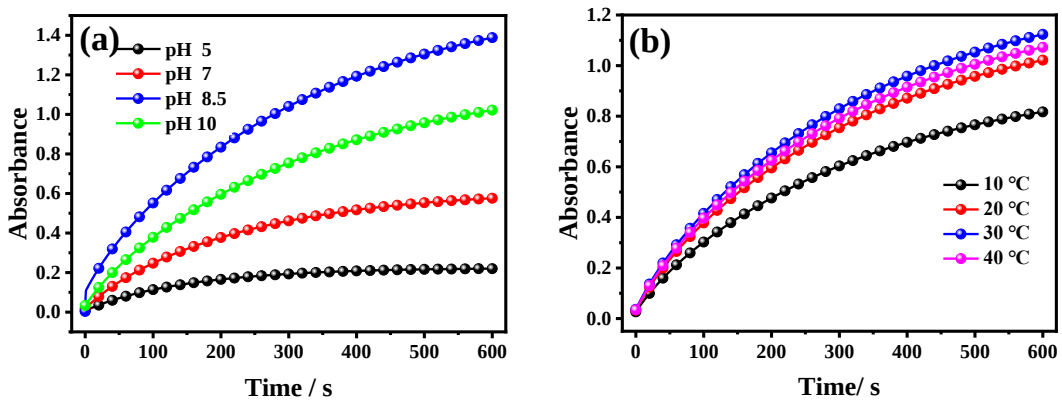

Fig. S8 Time-dependent absorbance spectra of TMB oxidation in presence of HSA@PDA/Fe nanocomposites and H_2O_2. The HSA@PDA/Fe nanocomposites were synthesized at different (a) pH values and (b) temperature. The total volume of the reaction mixture is 400 μL. All of the experiments were conducted in HAc-NaAc buffer (pH 4.5, 10 mM). The absorbances were collected at 652 nm.

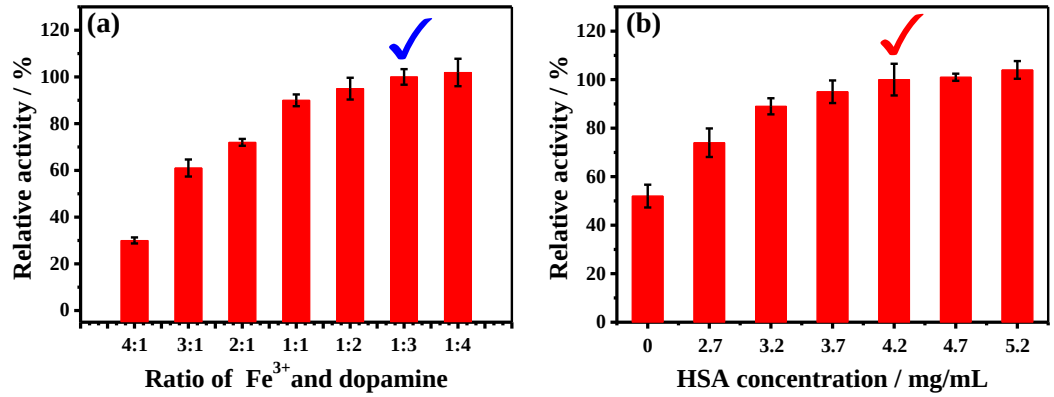

Fig. S9 Effects of (a) the ratio of Fe^{3+} and dopamine, (b) HSA concentration on the catalytic activity of HSA@PDA/Fe nanocomposites. (Insert: the tick represented the optimal conditions.) All of the experiments were conducted in HAc-NaAc buffer (pH 4.5, 10 mM). The error bars represented the standard deviation of three independent measurements. When one parameter changed, the others were under their optimal conditions.

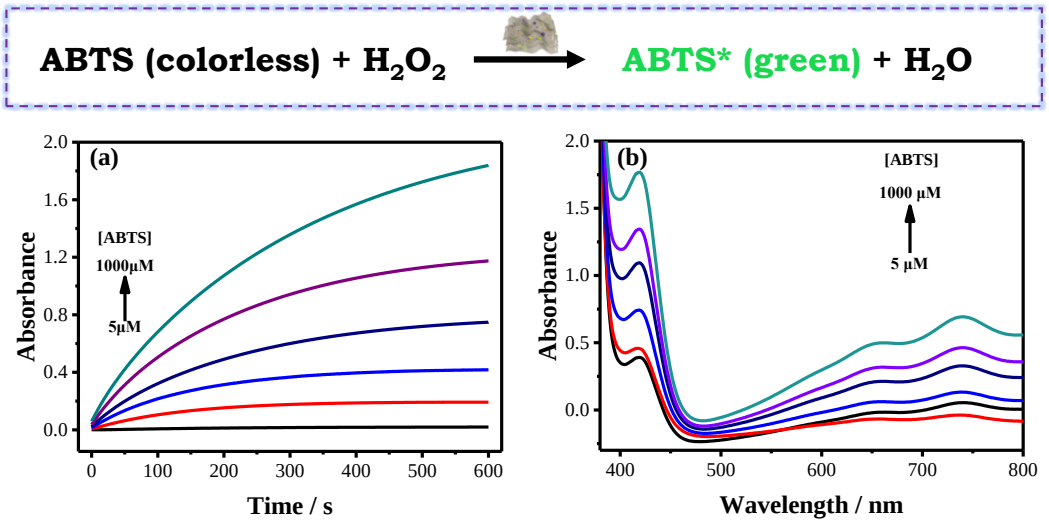

Figgure S10 (a) The absorption spectra, (b) Time-dependent absorbance spectra using HSA@PDA/FeNC (10 μg/mL). The reaction solution include H_2O_2 (1 mM) and ABTS with variable concentration of 5 μM, 10 μM, 50 μM, 100 μM, 500 μM and 1000 μM. The total volume of the reaction mixture was 400 μL. All of the experiments were conducted in 10 mM HAc-NaAc buffer, pH = 4.5, the absorbance at 418 nm.

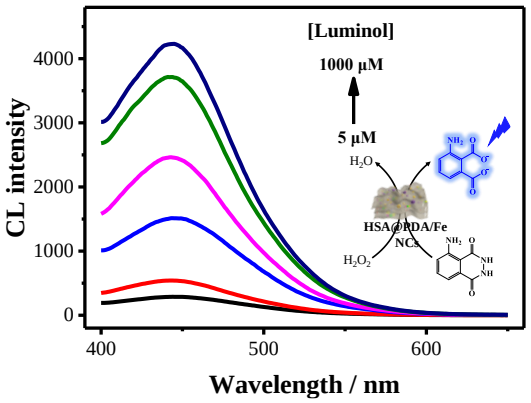

Fig. S11 Chemiluminescence spectra generated by the HSA@PDA/FeNCs catalyzed oxidation of different reaction solution. The reaction solution include H_2O_2 (1 mM) and luminol with variable concentration of 5 μM, 10 μM, 50 μM, 100 μM, 500 μM and 1000 μM. The total volume of the reaction mixture was 400 μL.

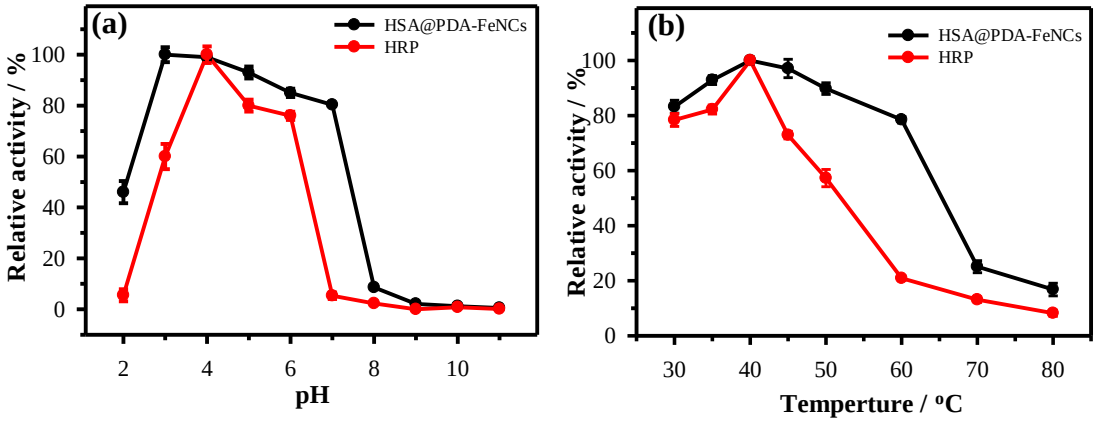

Fig. S12 Effects of (a) pH and (b) temperature on the catalytic activities of HSA@PDA/FeNCs (black line) and free HRP (red line). Experiments were carried out using HRP (10 μg/mL) or HSA@PDA/FeNCs(10 μg/mL). All reactions were implemented in HAc-NaAc buffer with TMB (1 mM) and H_2O_2 (1 mM).

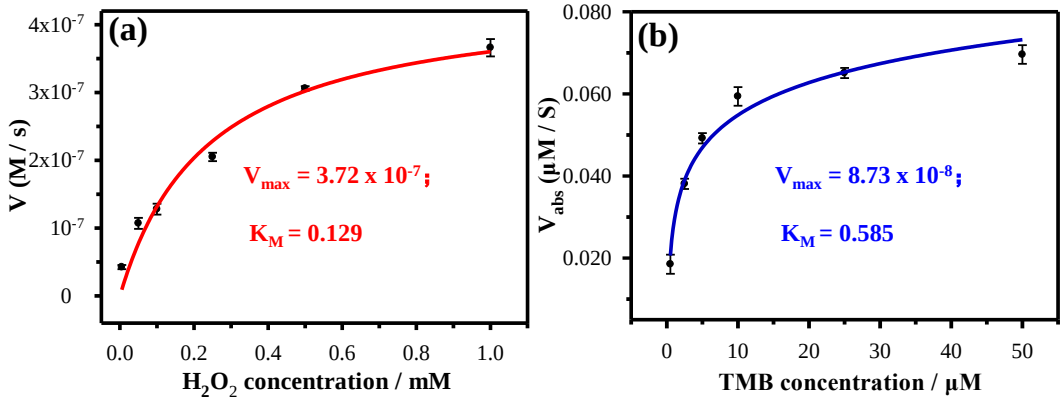

Fig. S13 Steady-state kinetic assay of HSA@PDA/Fe NCs for (a) H_2O_2 and (b) TMB. Experiments were carried out using HSA@PDA/FeNCs (10 μg/mL). All reactions were implemented in HAc-NaAc buffer (pH 4.5, 10 mM) with TMB (1 mM) and H_2O_2 (1 mM)

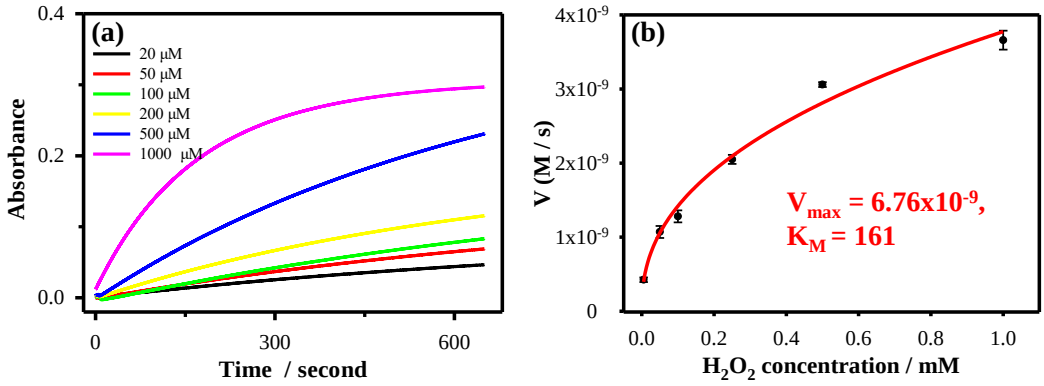

Fig. S14 (a) Time-dependent absorbance spectra and (b) the rates of solution in presence of Fe^{3+} (10 μg/mL). The reaction solution include TMB (1 mM) and H_2O_2 with variable concentration of 0.01 mM, 0.05 mM, 0.1 mM, 0.2 mM, 0.5 mM and 1 mM. The total volume of the reaction mixture was 400 μL. All of the experiments were conducted in 10 mM HAc-NaAc buffer, pH = 4.5, the absorbance at 652 nm.

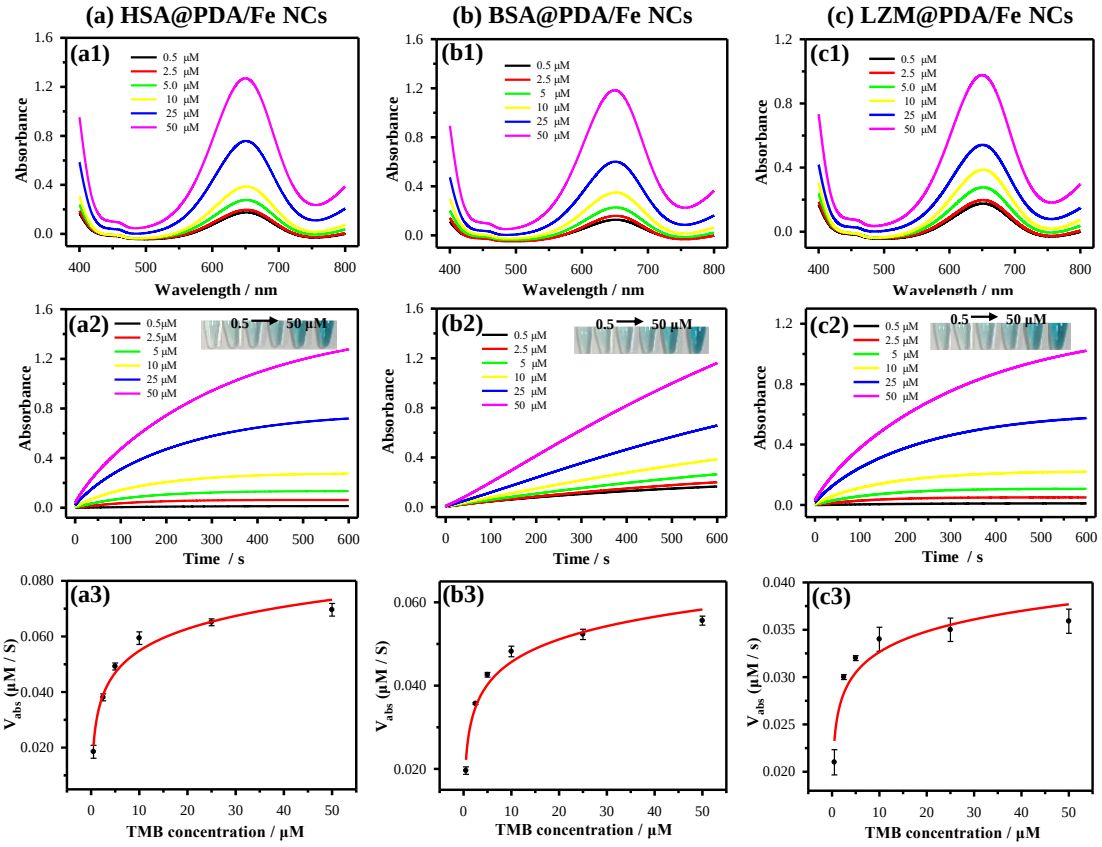

Fig. S15 The absorption spectra, time-dependent absorbance spectra and the rates of reaction was measured using (a) HSA@PDA/Fe, (b) BSA@PDA/Fe and (c) LZM@PDA/Fe nanocomposites (10 μg/mL).

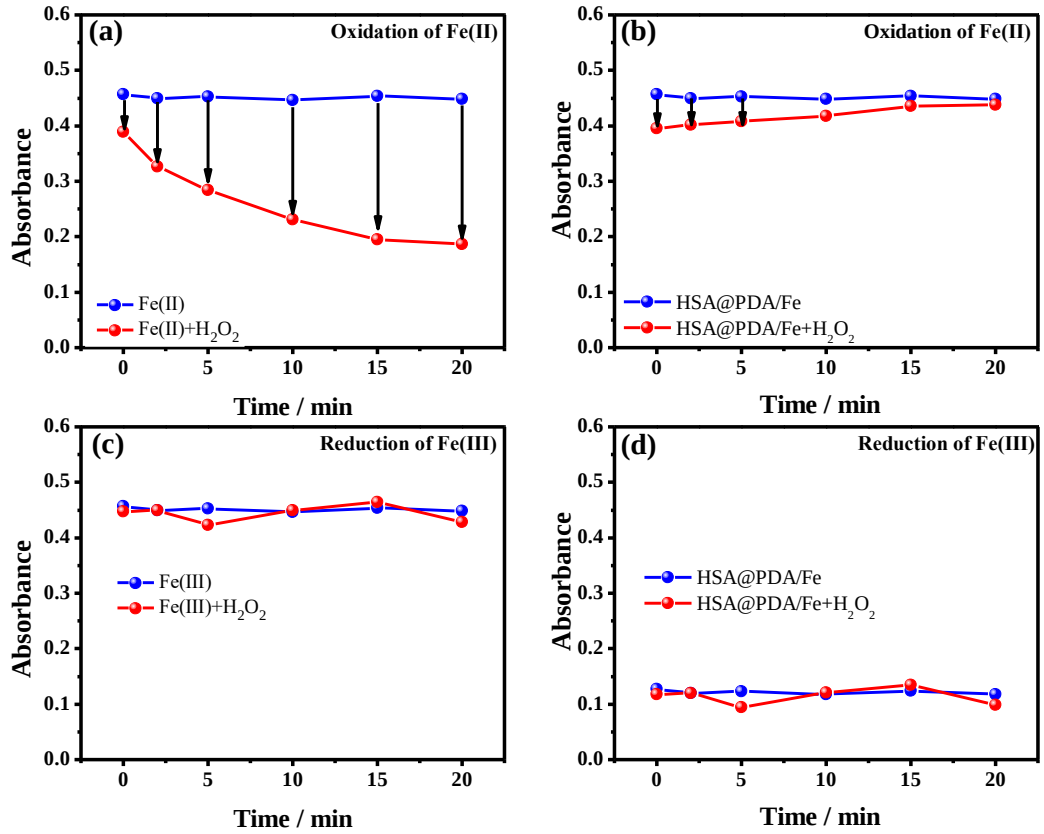

Fig. S16 Fe(II) concentration detection: (a) the absorbance of Fe(II) and Fe(II)+ H_2O_2, and (b) the absorbance of HSA@PDA/Fe nanocomposites and HSA@PDA/Fe nanocomposites+ H_2O_2, with the addition of 1,10-phenanthroline monohydrate. Fe(III) concentration detection: (c) the absorbance of Fe(III) and Fe(III)+ H_2O_2, and (d) the absorbance of HSA@PDA/Fe nanocomposites and HSA@PDA/Fe nanocomposites+ H_2O_2, with the addition of KSCN solution.

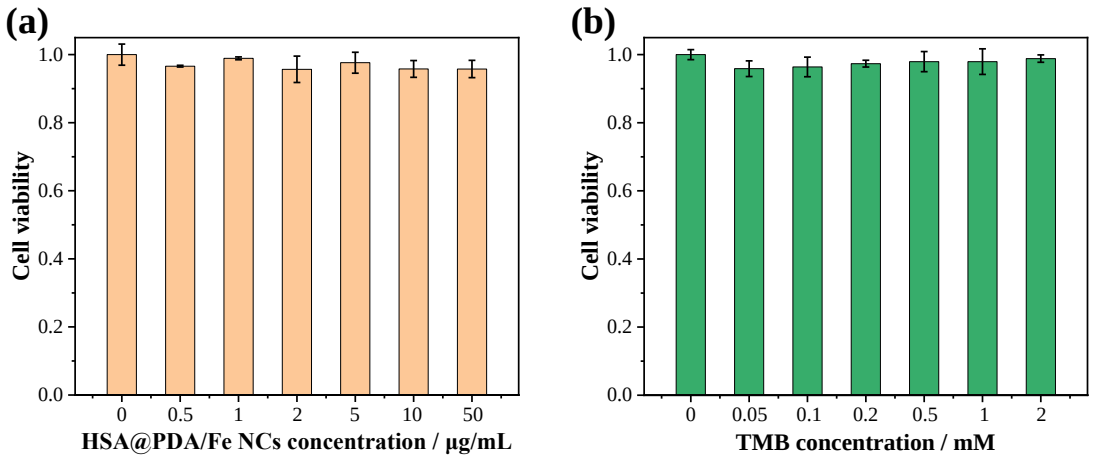

Fig. S17 MTT assay of the (A) HSA@PDA/Fe NCs and (B)TMB.

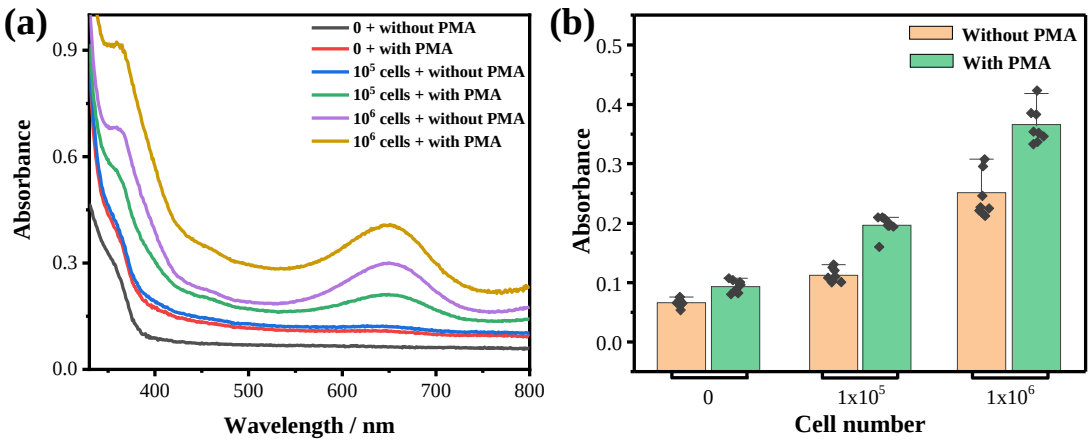

Fig. S18 (a) UV−vis absorption spectra and (b) absorbance values of the different number of SMCC-7721 cells incubated with or without PMA.

References

[1] Y. Sang, Y. Huang, W. Li, J. Ren and X. Qu, *Chem. Eur. J.*, 2018, **24**, 7259-7263.

[2] L. Gao, J. Zhuang, L. Nie, J. Zhang, Y. Zhang, N. Gu, T. Wang, J. Feng, D. Yang, S. Perrett and X. Yan, *Nat. Nanotechnol.*, 2007, **2**, 577-583.

[3] Y. Song, K. Qu, C. Zhao, J. Ren and X. Qu, *Adv. Mater*. 2010, *22*, 2206-2210.

[4] W. Shi, Q. Wang, Y. Long, Z. Cheng, S. Chen, H. Zheng and Y. Huang, *Chem. Commun.*, 2011, **47**, 6695-6697.

[5] R. Li, M. Zhen, M. Guan, D. Chen, G. Zhang, J. Ge, P. Gong, C. Wang and C. Shu, *Biosens. Bioelectron.*, 2013, **47**, 502-507.

[6] S. Zhu, X. E. Zhao, J. You, G. Xu and H. Wang, *Analyst*, 2015, **140**, 6398-6403.

[7] Z. Gao, M. Xu, L. Hou, G. Chen and D. Tang, *Anal. Chim. Acta.*, 2013, **776**, 79-86.

[8] M. S. Kim, S. Cho, S. H. Joo, J. Lee, S. K. Kwak, M. I. Kim and J. Lee, *ACS Nano*, 2019, **13**, 4312-4321.

[9] J. Mu, Y. Wang, M. Zhao and L. Zhang, *Chem. Commun.*, 2012, **48**, 2540-2542.

[10] P. Ling, Q. Zhang, T. Cao and F. Gao, *Angew. Chem. Int. Ed. Engl.,* 2018, **57**, 6819-6824.

[11] L. Huang, J. Chen, L. Gan, J. Wang and S. Dong, *Sci. Adv.*, 2019, **5**, eaav5490.

[12] T. Lin, L. Zhong, L. Guo, F. Fu and G. Chen, *Nanoscale,* 2014, **6**, 11856-11862.

[13] F. Yuan, H. Zhao, H. Zang, F. Ye and X. Quan, *ACS Appl. Mater. Interfaces,* 2016, **8**, 9855-9864.

[14] B. Tan, H. Zhao, W. Wu, X. Liu, Y. Zhang and X. Quan, *Nanoscale,* 2017, **9**, 18699-18710.

[15] P. Ju, Y. Yu, M. Wang, Y. Zhao, D. Zhang, C. Sun and X. Han, *J. Mater. Chem. B,* 2016, **4**, 6316-6325.

[16] T. Zhang, Y. Lu and G. Luo, *ACS Appl. Mater. Interfaces,* 2014, **6**, 14433-14438.

[17] Y. Dong, H. Zhang, Z. U. Rahman, L. Su, X. J. Chen, J. Hu and X. G. Chen, *Nanoscale,* 2012, **4**, 3969-3976.

[18] Y. Lu, W. C. Ye, Q. Yang, J. Yu, Q. Wang, P. P. Zhou, C. M. Wang, D. S. Xue and S. Q. Zhao, *Sensor. Actuat. B Chem.,* 2016, **230**, 721-730.

[19] X. Zhang, X. Bi, W. Di and W. Qin, *Sensor. Actuat. B Chem.*, 2016, **231**, 714-722.

[20] Y. Liu, Y. Zheng, Z. Chen, Y. Qin and R. Guo, *Small,* 2019, **15**, e1804987.

[21] H. Wei and E. Wang, *Anal. Chem.,* 2008, **80**, 2250-2254.

[22] Y. Jv, B. Li and R. Cao, *Chem. Commun.*, 2010, **46**, 8017-8019.

[23] M. I. Kim, J. Shim, T. Li, P. Lee and P. G. Park, *Chem. Eur. J.* 2011, **17**, 10700-10707.

[24] H. Cheng, L. Zhang, J. He, W. Guo, Z. Zhou, X. Zhang, S. Nie and H. Wei, *Anal. Chem.*, 2016, **88**, 5489-5497.

[25] Y. Huang, M. Zhao, S. Han, Z. Lai, J. Yang, C. Tan, Q. Ma, Q. Lu, J. Chen, X. Zhang, Z. Zhang, B. Li, B. Chen, Y. Zong and H. Zhang, *Adv. Mater.*, 2017, **29**, 1700102.

[26] X. He, L. Tan, D. Chen, X. Wu, X. Ren, Y. Zhang, X. Meng and F. Tang, *Chem. Commun.*, 2013, **49**, 4643-4645.

[27] Y. Liu, M. Yuan, L. Qiao and R. Guo, *Biosens. Bioelectron.*, 2014, **52**, 391-396.